| 刊行書籍または雑誌名<br>（雑誌のときは雑誌名　巻頁数　論文名） | 刊行年 | 執筆者氏名 |
|---|---|---|
| Arch Ophthalmol. 2011 Dec;129(12):1629-30.<br>Human herpesvirus 8 in corneal endotheliitis resulting in graft failure after penetrating keratoplasty refractory to allograft rejection therapy. | 2011 | Inoue T, Takamatsu F, Kubota A, Hori Y, Maeda N, Nishida K. |
| Cornea. 2011 Oct;30 Suppl 1:S50-3.<br>Chandelier illumination for use during descemet stripping automated endothelial keratoplasty in patients with advanced bullous keratopathy. | 2011 | Inoue T, Oshima Y, Hori Y, Maeda N, Nishida K. |
| Tissue Eng Part A. 2011 Sep;17(17-18):2213-9.<br>A novel gelatin hydrogel carrier sheet for corneal endothelial transplantation. | 2011 | Watanabe R, Hayashi R, Kimura Y, Tanaka Y, Kageyama T, Hara S, Tabata Y, Nishida K. |
| Genes Cells. 2011 Mar;16(3):273-81.<br>Neural crest-derived multipotent cells in the adult mouse iris stroma. | 2011 | Kikuchi M, Hayashi R, Kanakubo S, Ogasawara A, Yamato M, Osumi N, Nishida K. |

| 論文タイトル<br>（雑誌名、巻頁数） | 刊行年 | 刊行書店名 | 執筆者氏名 |
|---|---|---|---|
| 再生医療の産業化に対して必要な仕組みとは<br>（再生医療，vol.10, No.2，p111-124） | 2011 | メディカルレビュー社 | 桜田一洋、森山剛、西田幸二、畠賢一郎、中西淳 |
| 円錐角膜に対する全層角膜移植と深層表層角膜移植の術後経過の比較<br>（臨床眼科，第 65 巻，第 9 号，p1413-1417） | 2011 | 医学書院 | 植松恵、横倉俊二、大家義則、目黒泰彦、針谷威寛、布施昇男、西田幸二 |
| 論点—角膜内皮移植の課題<br>（眼科手術，vol.24，No.4，p389-390） | 2011 | メディカル葵出版 | 西田幸二 |
| 【幹細胞治療-基礎研究の進歩と臨床応用-】 臨床応用の進歩　眼科角膜領域再生医療<br>（日本臨床，69 巻，12 号，p2235-2240） | 2011 | 日本臨床社 | 辻川元一、西田幸二 |
| 培養上皮細胞シート移植（眼科最新手術）‥（角結膜）<br>（眼科，53 巻，10 号，p1451-1455） | 2011 | 金原出版株式会社 | 相馬剛至、西田幸二 |
| 角膜移植（眼球提供から移植まで）<br>（眼科，53 巻，12 号，p1709-1713） | 2011 | 金原出版株式会社 | 相馬剛至 |
| 角膜内皮移植（DSAEK）　DSAEK のドナー挿入法<br>（眼科手術，vol.24，No.4，p401-403） | 2011 | メディカル葵出版 | 相馬剛至、西田幸二 |
| 「上皮幹細胞」<br>MSD（メディカル・サイエンス・ダイジェスト）Vol.37, No8, p308-311 | 2011 | ニューサイエンス社 | 林竜平 |
| 「幹細胞を用いた角膜再生医療」－再生医療－<br>（再生医療，Vol10, No.2，p104-108） | 2011 | メディカルレビュー社 | 林竜平、西田幸二 |

## RESEARCH LETTERS

### Human Herpesvirus 8 in Corneal Endotheliitis Resulting in Graft Failure After Penetrating Keratoplasty Refractory to Allograft Rejection Therapy

Although corneal allograft rejection after penetrating keratoplasty responds to corticosteroids, in some edematous grafts, herpes simplex virus, varicella-zoster virus, or cytomegalovirus causes corneal endotheliitis refractory to steroids and leads to graft failure without appropriate antiviral therapy.[1] However, other cases with idiopathic corneal endotheliitis refractory to steroids remain to be studied. Human herpesvirus 8 (HHV-8) is associated with neoplastic diseases.[2,3] We report graft failure after penetrating keratoplasty, with aqueous humor positive for HHV-8 DNA by real-time polymerase chain reaction.

**Report of a Case.** A 56-year-old man who underwent penetrating keratoplasty in his left eye 5 years previously for recurrent keratouveitis and total bullous keratopathy manifested ocular pain and sudden decreased vision in that eye (best-corrected visual acuity, 20/100; intraocular pressure, 25 mm Hg). Examination showed severe localized corneal edema mainly in the graft, ciliary injection, keratic precipitates, and mild anterior chamber inflammation (**Figure**). Because the edema was associated with minimal stromal infiltrates and endothelial dysfunction, corneal endotheliitis was diagnosed. The fundus, optic nerve, and fellow eye were normal. Serologic tests were positive for HHVs (enzyme immunoassay results: herpes simplex virus IgG, 42.7; varicella-zoster virus IgG, 38.1; Epstein-Barr virus viral capsid antigen–IgG, 11.0; and cytomegalovirus IgG, 25.8; fluorescence antibody method results: HHV-6 IgG, 10.0; HHV-7 IgG, 10.0) and negative for human immunodeficiency virus. No HHV-8 serologic test is available in Japan. The patient had diabetes mellitus and hypertension but did not have cancer or immunosuppressive disease. Based on ocular manifestations, corneal allograft rejection was suspected; however, topical and systemic steroids (betamethasone, 0.1%, hourly, and intravenous methylprednisolone hemisuccinate, 125 mg 3 times total) and ocular antihypotensive therapy (timolol maleate, 0.5%, twice daily, and oral acetazolamide, 500 mg/d) were ineffective. Allograft rejection and herpetic corneal endotheliitis can have similar appearances. Resistance to rejection therapy suggested herpetic infection as another diagnostic option. An aqueous humor sample subjected to polymerase chain reaction for herpes simplex virus 1 or 2, varicella-zoster virus, Epstein-Barr virus, cytomegalovirus, and HHV-6, HHV-7, or HHV-8[1] detected only HHV-8 DNA (*ORF26* gene, $2.5 \times 10^5$ copies/mL).[4] Thirty aqueous humor samples from patients with cataract but without keratitis contained no HHV-8 DNA. Only HHV-8 detection suggested that HHV-8 caused corneal endotheliitis after penetrating keratoplasty; however, anti–HHV-8 treatment was unavailable.

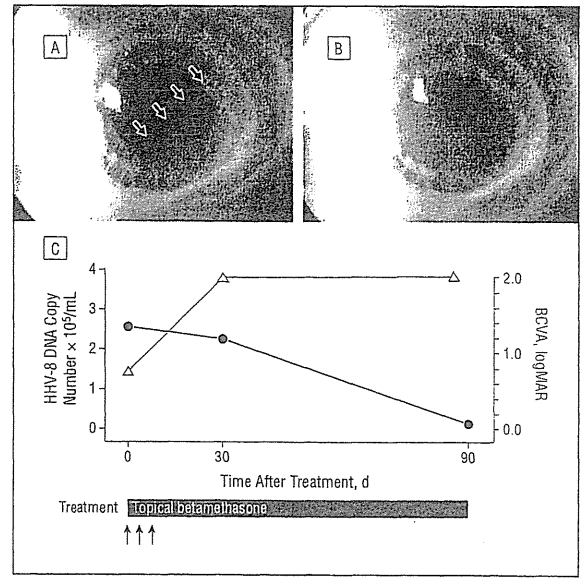


**Figure.** Relationship between the therapeutic outcome with allograft rejection therapy and human herpesvirus 8 (HHV-8) copy number. A, Slitlamp photograph shows localized corneal edema on a corneal graft with keratic precipitates (arrows) and severe injection before treatment (day 0). B, Slitlamp photograph shows that the corneal edema gradually progressed and resulted in total bullous keratopathy 4 weeks after treatment (day 28). C, Although allograft rejection therapy continued, the corneal edema progressed gradually to total bullous keratopathy resulting in graft failure, and the HHV-8 copy number had not decreased by 4 weeks after treatment. When the HHV-8 copy number reached an undetectable level, the visual acuity and the clinical appearance of the bullous keratopathy 3 months after treatment (day 90) did not improve. Arrows indicate administration of intravenous methylprednisolone hemisuccinate, 125 mg; BCVA, best-corrected visual acuity.

Despite allograft rejection therapy, corneal edema progressed to total bullous keratopathy and graft failure and the HHV-8 copy number did not decrease by 4 weeks after treatment ($2.2 \times 10^5$ copies/mL) (Figure). Because inflammation gradually resolved and the intraocular pressure decreased to less than 15 mm Hg without treatment, antiallograft rejection therapy ended after 3 months when no HHV-8 copies were detected. The best-corrected visual acuity did not recover to 20/2000 and the corneal graft did not improve. There has been

no recurrence 2 years after treatment; the patient awaits corneal regrafting.

Comment. Although HHV-8 causes neoplastic disease (Kaposi sarcoma, multicentric Castleman disease, and primary effusion lymphoma in an immunocompromised host), HHV-8–related clinical manifestations are not well defined.[2,3,5] To our knowledge, this is the first report of corneal endotheliitis positive for HHV-8 leading to graft failure in an immunocompetent patient.

It is uncertain whether HHV-8 was the cause because polymerase chain reaction detection does not necessarily mean that HHV-8 caused the clinical manifestations of corneal endotheliitis.

Because anti–HHV-8 therapy was unavailable, graft failure occurred with only antiallograft rejection therapy. Expression of HHV-8 DNA in the aqueous was high in the active inflammatory phase (before and 3 weeks after treatment) but not in the stable phase (3 months after treatment). Polymerase chain reaction results for HHV-1 through HHV-7 at 3 weeks and 3 months after treatment indicated no positivity for HHVs without antiviral therapy throughout the therapy course. Because other HHVs[6] cause corneal endotheliitis, HHV-8 may be a candidate. These findings suggest that HHV-8 infection may play a role in corneal endotheliitis leading to graft failure. Investigations about specific anti–HHV-8 therapy or the latency of HHV-8 are needed.

*Tomoyuki Inoue, MD*
*Fumihiko Takamatsu, MS*
*Akira Kubota, MD*
*Yuichi Hori, MD*
*Naoyuki Maeda, MD*
*Kohji Nishida, MD*

**Author Affiliations:** Department of Ophthalmology, Osaka University Medical School, Suita (Drs Inoue, Maeda, and Nishida and Mr Takamatsu), Department of Ophthalmology, Sumitomo Hospital, Osaka (Drs Inoue and Kubota), and Department of Ophthalmology, Toho University Sakura Medical Center, Sakura (Dr Hori), Japan.
**Correspondence:** Dr Inoue, Department of Ophthalmology, Sumitomo Hospital, 5-3-20 Nakanoshima, Kita-ku, Osaka 530-0005, Japan (tomonoue@gmail.com).
**Financial Disclosure:** None reported.
**Funding/Support:** This study was supported by a research grant from the Osaka Eye Bank Foundation, Suita, Japan (Dr Inoue).

1. Suzuki T, Ohashi Y. Corneal endotheliitis. *Semin Ophthalmol.* 2008;23(4):235-240.
2. Levy JA. Three new human herpesviruses (HHV6, 7, and 8). *Lancet.* 1997;349(9051):558-563.
3. Miyagawa H, Yamanishi K. The epidemiology and pathogenesis of infections caused by the high numbered human herpesviruses in children: HHV-6, HHV-7 and HHV-8. *Curr Opin Infect Dis.* 1999;12(3):251-255.
4. Maeda N, Yamashita Y, Kimura H, Hara S, Mori N. Quantitative analysis of herpesvirus load in the lymph nodes of patients with histiocytic necrotizing lymphadenitis using a real-time PCR assay. *Diagn Mol Pathol.* 2006;15(1):49-55.
5. Verma V, Shen D, Sieving PC, Chan CC. The role of infectious agents in the etiology of ocular adnexal neoplasia. *Surv Ophthalmol.* 2008;53(4):312-331.
6. Inoue T, Kandori M, Takamatsu F, Hori Y, Maeda N. Corneal endotheliitis with quantitative polymerase chain reaction positive for human herpesvirus 7. *Arch Ophthalmol.* 2010;128(4):502-503.

## The 10-Year Incidence of Glaucoma Among Patients With Treated and Untreated Ocular Hypertension

The Ocular Hypertension Treatment Study has shown that medical treatment of ocular hypertension (OHT) reduces the incidence of primary open-angle glaucoma (POAG) at 5 years by more than 50%.[1] The greatest absolute reduction in incidence occurs among those at highest risk based on baseline age, intraocular pressure, central corneal thickness, vertical cup-disc ratio, and pattern standard deviation. In clinical practice, most patients with OHT are followed up for longer than 5 years.[1-3] To help clinicians and patients make decisions about the benefit of early medical treatment and the frequency of examinations, we have calculated the 10-year incidence of POAG under 2 scenarios: treated, ie, medical treatment for 10 years, and untreated, ie, no medical treatment for 10 years.

Methods. The Ocular Hypertension Treatment Study randomized 1636 participants to either medical treatment or observation. After a mean follow-up of 7.5 years, observation participants were then also offered medication. Both groups were followed up for an additional 5.5 years. To estimate the incidence of POAG for the scenario of treated for 10 years, we used data from the medication group. To estimate the incidence of POAG for the scenario of untreated for 10 years, we used untreated data from the observation group. For each scenario, a parametric proportional hazards model was fit while including the 5 aforementioned baseline predictors.[2,3] The baseline hazard function in each model used 4-knot restricted cubic splines, with the knots chosen as the 5th, 33rd, 67th, and 95th percentiles of the uncensored survival times.[4] The 95% CIs were obtained using bootstrap methods from 1000 bootstrap runs resampling the original data with replacement. All analyses were performed using the R version 2.9.2 statistical package (R Foundation for Statistical Computing, Vienna, Austria).

Results. The 10-year incidence of POAG in participants with OHT is reported by baseline levels of risk (tertiles) and by ethnicity (**Table**). Medical treatment for 10 years reduced the incidence of POAG by about 50% at all 3 tertiles of risk. The absolute reduction was greatest in the highest tertile of risk (23%, from 42% to 19%) and lowest in the lowest tertile of risk (3%, from 7% to 4%). Within each tertile of risk, incidences of POAG among African American participants and those who are not African American were similar.

Comment. Topical medication for OHT reduces the 10-year incidence of POAG by 50% at all 3 tertiles of risk for the entire group as well as African American participants.[5] The absolute reduction in incidence of POAG was greatest in the group at the highest tertile of baseline risk. The incidence of POAG in participants with OHT appears to be roughly linear during the first 10 years. It is unknown whether this finding can be extrapolated to 20 years of follow-up or more.

# Chandelier Illumination for Use During Descemet Stripping Automated Endothelial Keratoplasty in Patients With Advanced Bullous Keratopathy

*Tomoyuki Inoue, MD,* Yusuke Oshima, MD,† Yuichi Hori, MD,‡ Naoyuki Maeda, MD,† and Kohji Nishida, MD†*

**Abstract:** We demonstrate a technique that uses chandelier illumination during Descemet stripping automated endothelial keratoplasty (DSAEK) in cases of severe bullous keratopathy. A chandelier illumination fiber inserted through the corneal side port provides sclerotic scattering-like illumination from the sclerocorneal margin and endoillumination from the anterior chamber, resulting in excellent visibility for Descemet stripping and intraocular manipulation without obstruction from a hazy cornea. In cases complicated by dense cataract, the chandelier fiber can be inserted transconjunctivally into the pars plana, providing sufficient retroillumination to perform phacoemulsification with intraocular lens implantation combined with Descemet stripping for a DSAEK triple procedure. Because of the powerful illumination and hands-free nature of the chandelier fiber, the Descemet membrane can be visualized clearly and stripped as 1 sheet without inadvertent complications. We have developed a new 25-gauge illuminated anterior chamber maintainer comprising a 25-gauge infusion cannula through which a 29-gauge chandelier fiber probe passes. Because of the resulting bright illumination and adequate irrigation flow, excellent visibility with stable anterior chamber maintenance can be concurrently obtained for Descemet stripping, endothelial graft insertion, and subsequent intraocular manipulations without the need for biological staining or ophthalmic viscosurgical products, even in patients with severe corneal haze. This technique and new device facilitates safe and simple intraocular manipulation during DSAEK and encourages surgeons to perform DSAEK in challenging cases.

**Key Words:** bullous keratopathy, chandelier illumination, Descemet stripping automated endothelial keratoplasty, infusion cannula

(*Cornea* 2011;30(Suppl. 1):S50–S53)

Descemet stripping automated endothelial keratoplasty (DSAEK) is considered the first treatment of choice for endothelial diseases, such as Fuchs dystrophy and pseudophakic bullous keratopathy. The technique displaces the diseased host endothelium and the Descemet membrane through a small incision without full-thickness corneal penetration and is an alternative to the conventional penetrating keratoplasty (PKP). DSAEK is a minimally invasive procedure that offers several advantages over conventional PKP, including better preservation of host corneal biomechanical properties and structural integrity, minimally induced changes in corneal astigmatism, and fewer ocular surface complications, thus resulting in rapid visual recovery.[1–6] However, this promising new procedure for treating advanced endothelial diseases is still considered challenging because of difficulties with intraocular visualization and manipulation through very hazy corneas.[2,7,8]

To overcome these problems, we focused on intraocular illumination using a chandelier illumination system for DSAEK to facilitate clear intraocular visibility, safe Descemet stripping, and sequential manipulation through a hazy cornea. In this article, we demonstrate chandelier illumination-assisted DSAEK for the treatment of advanced bullous keratopathy, including 2 illumination approaches combined with or without cataract surgery.[9] We also describe a newly developed device for anterior segment surgery, an illuminated anterior chamber maintainer.[10]

## CHANDELIER ILLUMINATION SYSTEM

The chandelier illumination system provides a wide-angle intraocular illuminating system originally used for vitreous surgery. A commercially available, self-retaining, 25-gauge (0.5 mm) or 27-gauge (0.35 mm) chandelier illumination fiber (Synergetics USA, Inc., O'Fallon, MO) with a Photon II mercury vapor light source was used in this study.[9,11,12]

## SUBJECTS FOR CHANDELIER ILLUMINATION-ASSISTED DSAEK

The chandelier illumination technique was performed only in cases with severe corneal haze, through which intraocular visibility could not be obtained with conventional microscopic illumination. In this challenging situation, 2 different chandelier illuminating approaches, anterior chamber illumination and retroillumination, can be introduced, depending on whether DSAEK is performed with or without cataract surgery. Anterior chamber

From the *Department of Ophthalmology, Sumitomo Hospital, Osaka, Japan; †Department of Ophthalmology, Osaka University Medical School, Suita, Japan; and ‡Department of Ophthalmology, Toho University Sakura Medical Center, Sakura, Japan.

The authors state that they have no financial or conflicts of interest to disclose.

Reprints: Tomoyuki Inoue, Department of Ophthalmology, Sumitomo Hospital, Osaka 530-0005, Japan (e-mail: tomonoue@gmail.com).

illumination is selected for DSAEK in pseudophakia cases, and retroillumination is selected for DSAEK combined with cataract surgery. No cases of long-standing bullous keratopathy with dense stromal scaring were selected because these are more suitable candidates for PKP.

## ANTERIOR CHAMBER ILLUMINATION FOR DSAEK IN PSEUDOPHAKIA

In pseudophakic eyes with severe corneal haze, light from a conventional surgical microscope is reflected and hinders visibility inside the eye. In pseudophakia, a 25-gauge self-retaining chandelier fiber is set at the corneal limbus with the tip inside the anterior chamber (approximately 2–3 mm) through a small side port incision created by a 25-gauge microvitreoretinal blade inferonasally for the best visibility of the corneal endothelial layer.[9] Because of the hands-free and self-retaining nature of the chandelier fiber, bimanual manipulation can be performed easily. In contrast to the poor visibility with conventional microscopic illumination, sclerotic scattering-like illumination from the sclerocorneal margin and endoillumination from the anterior chamber generated by the chandelier illumination fiber offer sufficient lighting to clearly view the anterior chamber and the corneal endothelial layer, despite a hazy cornea. Therefore, Descemet stripping from the recipient stroma and subsequent manipulation can be easily visualized and safely carried out under chandelier illumination through a hazy cornea without biological staining to enhance membrane visualization (Fig. 1). The Descemet membrane can be stripped as a single sheet, which eliminates concerns about residual membrane adhering to the recipient stroma. Subsequent manipulation of DSAEK, such as donor graft insertion and centering and apposition of the donor graft sheet to the recipient, can still be visualized using chandelier illumination. After removing the chandelier fiber from the corneal side port, the corneal wound can be sealed easily with slight corneal stromal hydration at the end of the surgery.

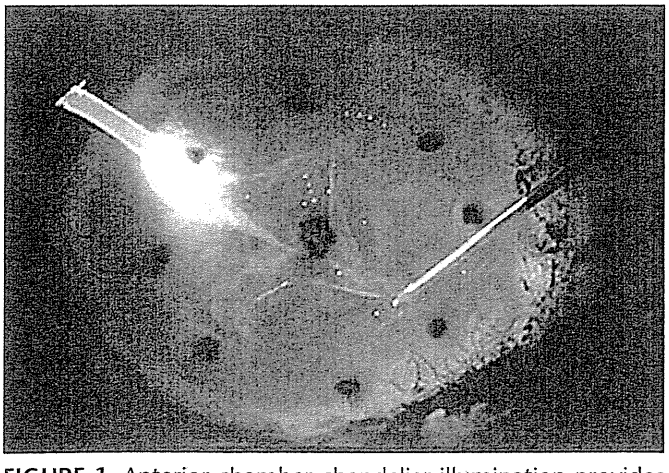

**FIGURE 1.** Anterior chamber chandelier illumination provides excellent intraocular visualization. All manipulations used in the anterior chamber for Descemet stripping and the stripped endothelial membrane itself can be visualized through a hazy cornea.

## RETROILLUMINATION FOR DSAEK COMBINED WITH CATARACT SURGERY

In patients with bullous keratopathy combined with dense cataracts, simultaneous DSAEK and phacoemulsification with intraocular lens (IOL) implantation, the so-called triple procedure, has recently been reported to be a beneficial treatment option.[9] Combined DSAEK and phacoemulsification is technically challenging because cataract surgery must be performed through a cloudy cornea.[13] The aforementioned anterior chamber illumination technique is insufficient for performing cataract surgery because the scattered reflection from the corneal haze will interfere with intracapsular visibility. A chandelier fiber set at the pars plana can be used for patients with a severe haze in the cornea requiring the triple procedure. After retrobulbar anesthesia, a 25-gauge chandelier fiber is inserted transconjunctivally into the vitreous cavity through a sclerotomy using a 25-gauge needle at 3.5 mm posterior to the corneal limbus. The self-retaining chandelier stays in the inferotemporal pars plana region by virtue of its design, without the need for sutures. Retroillumination from the posterior side generated by the chandelier fiber and mercury vapor light source provides excellent intraocular visibility, resulting in safer intracapsular manipulation during phacoemulsification, and IOL insertion able to be performed without obstruction by the hazy cornea (Fig. 2), as previously described.[12] By changing the position of the chandelier fiber after cataract surgery, chandelier retroillumination can also provide excellent intraocular visibility during subsequent DSAEK despite a hazy cornea. Retroillumination offers sufficient lighting to safely perform intracapsular manipulation during phacoemulsification and IOL insertion, as well as Descemet stripping (Fig. 3) and subsequent manipulation by DSAEK. The Descemet membrane can be easily visualized and stripped successfully in 1 sheet. At the end of the surgery, the tip of the chandelier fiber is removed from the pars plana, and the scleral wound self-seals without requirement for sutures.

## DEVELOPMENT OF A CHANDELIER-ILLUMINATED ANTERIOR CHAMBER MAINTAINER

Illuminating the anterior chamber using chandelier illumination fibers originally intended for vitreous surgery is inconvenient during DSAEK, requiring an additional corneal side port and an infusion port to maintain the anterior chamber.[10] A bright wide-angle illumination from the chandelier probe can reflect glare into the surgeon's eyes and thermal burns can occur around the corneal side port. We developed an illuminated anterior chamber maintainer for surgery, with several advantages over the conventional chandelier fibers for DSAEK and other anterior segment surgeries.

**FIGURE 2.** Chandelier retroillumination from the posterior side provides sufficient lighting to view the anterior lens capsule clearly despite the hazy cornea, making it possible to perform capsulorhexis.

A stainless steel infusion tube attachment comprising a beveled 25-gauge infusion cannula with a footplate was fitted to a transparent infusion tube. A flexible 29-gauge chandelier microfiber was then passed through the infusion tube and the 25-gauge infusion cannula, with 0.5 mm of the cone-shaped tip of the optical microfiber protruding from the tip of the infusion cannula (Fig. 4). A flat footplate and an opaque malleable sleeve covering the transparent infusion tube maintain the position of the illuminated infusion line at the corneal limbus. The inner chandelier microfiber that passes through the infusion tube branches in the middle. The distal end can be connected to a xenon or mercury vapor light source to enhance the maximum illumination output. The distal end of the infusion line is connected to an irrigation bottle and at the appropriate bottle height draws irrigation fluid through the infusion line into the anterior chamber.

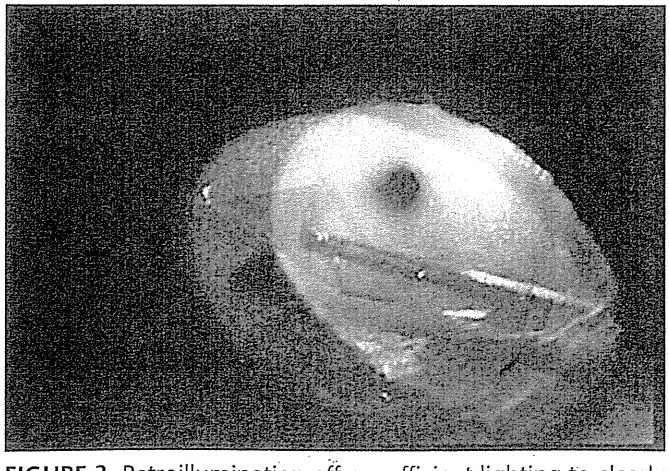

**FIGURE 3.** Retroillumination offers sufficient lighting to clearly view the anterior chamber through a hazy cornea for Descemet stripping.

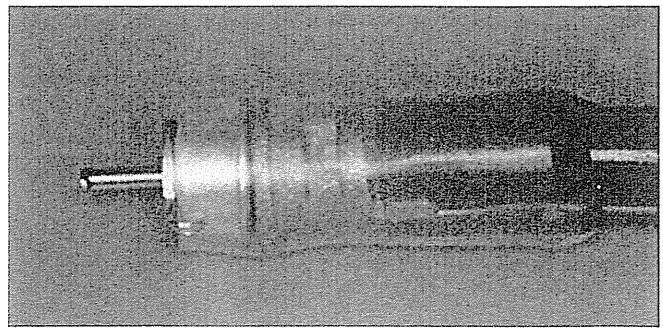

**FIGURE 4.** The illuminated anterior chamber maintainer. A chandelier microfiber is passed through the infusion tube and cannula with the cone-shaped tip of the optical microfiber protruding from the tip of the infusion cannula.

## APPLICATION OF A CHANDELIER-ILLUMINATED ANTERIOR CHAMBER MAINTAINER FOR DSAEK

During the surgery, a 25-gauge cannula of an illuminated anterior chamber maintainer is inserted into the anterior chamber through the corneal side port and anchored at the corneal limbus.[10] The infusion fiber connected to the irrigation bottle is self-retaining and supplies irrigation fluid into the anterior chamber through the 25-gauge infusion cannula. Combined with a mercury vapor light source, the 29-gauge chandelier probe provided optimal illumination to facilitate visibility of the corneal endothelial layer and the anterior chamber. All surgical manipulations, the instruments used in the anterior chamber for Descemet stripping, and the stripped endothelial membrane itself can be easily visualized despite the hazy cornea. The anterior chamber depth is maintained by the continuous irrigation flow through the infusion cannula, even during insertion of the endothelial donor graft through a 4-mm sclerocorneal wound. There is no

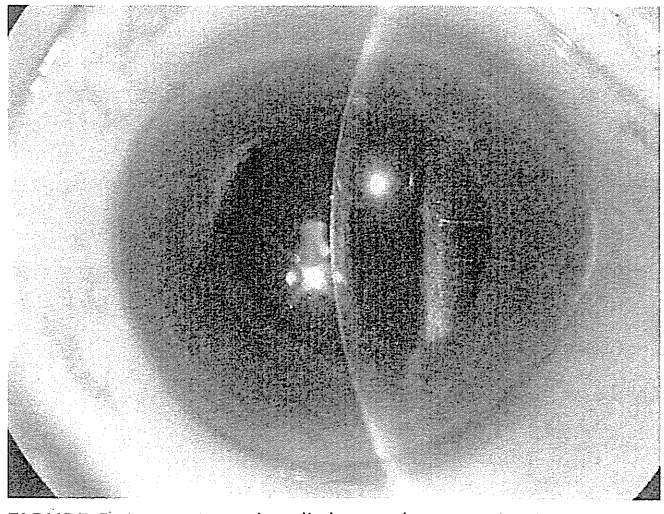

**FIGURE 5.** A postoperative slit-lamp photograph of an eye that underwent DSAEK under chandelier retroillumination shows a clear cornea 5 weeks after the surgery. The visual acuity improved from 0.1 to 1.0.

need for use of ophthalmic viscosurgical products to maintain space for surgical maneuvers performed during Descemet stripping and subsequent procedures. Because of its bifunctionality, anterior chamber illumination and irrigation can be achieved concurrently by inserting the device through a side port. The 25-gauge stainless infusion cannula covering the chandelier fiber probe is insulated to prevent thermal burn–induced corneal damage and minimize glare.

## CONCLUSIONS

Postoperatively, corneal clarity in patients with advanced bullous keratopathy can be restored successfully through anterior chamber chandelier illumination-assisted DSAEK (Fig. 5), the chandelier retroillumination-assisted triple procedure, or DSAEK with the illuminated anterior chamber maintainer, without encountering complications associated with this technique. The host cornea will recover to a normal range of thickness, and the donor endothelial graft sheet will successfully attach to the recipient stroma, as confirmed by anterior segment optical coherence tomography.

Descemet stripping might not be a critical procedure in every case, especially in those with a normal Descemet membrane or those in the early stages of endothelial decompensation without fibrotic changes in the Descemet membrane.[14] However, in advanced bullous keratopathy, such as that induced by argon laser iridectomy, bullous keratopathy is generally more severe than that caused by Fuchs corneal dystrophy and is often complicated by fibrotic changes in the Descemet membrane.[15,16] Inadequate Descemet membrane stripping that leaves fibrotic remnants adhering to the recipient stroma could cause poor donor graft adhesion, resulting in postoperative graft failure.[15] Stripping the diseased Descemet membrane in 1 sheet without remnants on the recipient stroma is critical for preventing this complication in cases of advanced bullous keratopathy with dense corneal haze.

The chandelier illumination technique is highly compatible with DSAEK. Chandelier illumination using anterior illumination and retroillumination techniques provides excellent visibility of the anterior chamber and corneal endothelial side through a hazy cornea. Bimanual manipulation during DSAEK can be easily performed because of the hands-free and self-retaining nature of the chandelier illumination fibers. Clear intraocular visibility obtained by the chamber illumination eliminates the need for epithelial removal[2] and biological staining[4,7] to enhance visibility through hazy corneas, thereby simplifying procedures and minimizing surgical trauma during DSAEK. This chandelier illumination technique and the newly developed device described above facilitate safe and simple intraocular manipulation, including complete stripping of the Descemet membrane in 1 sheet, encouraging surgeons to perform DSAEK in challenging cases.

## REFERENCES


1. Price FW Jr, Price MO. Descemet's stripping with endothelial keratoplasty in 50 eyes: a refractive neutral corneal transplant. *J Refract Surg*. 2005;21:339–345.
2. Price FW Jr, Price MO. Descemet's stripping with endothelial keratoplasty in 200 eyes: early challenges and techniques to enhance donor adherence. *J Cataract Refract Surg*. 2006;32:411–418.
3. Gorovoy MS. Descemet-stripping automated endothelial keratoplasty. *Cornea*. 2006;25:886–889.
4. Mearza AA, Qureshi MA, Rostron CK. Experience and 12-month results of Descemet-stripping endothelial keratoplasty (DSEK) with a small-incision technique. *Cornea*. 2007;26:279–283.
5. Koenig SB, Covert DJ. Early results of small-incision Descemet's stripping and automated endothelial keratoplasty. *Ophthalmology*. 2007;114:221–226.
6. Chen ES, Terry MA, Shamie N, et al. Descemet-stripping automated endothelial keratoplasty: six-month results in a prospective study of 100 eyes. *Cornea*. 2008;27:514–520.
7. Price MO, Price FW Jr. Endothelial keratoplasty technique for aniridic aphakic eyes. *J Cataract Refract Surg*. 2007;33:376–379.
8. Kobayashi A, Yokogawa H, Sugiyama K. Descemet stripping with automated endothelial keratoplasty for bullous keratopathies secondary to argon laser iridotomy-preliminary results and usefulness of double-glide donor insertion technique. *Cornea*. 2008;27(suppl 1):S62–S69.
9. Inoue T, Oshima Y, Shima C, et al. Chandelier illumination to complete Descemet stripping through severe hazy cornea during Descemet-stripping automated endothelial keratoplasty. *J Cataract Refract Surg*. 2008;34:892–896.
10. Inoue T, Oshima Y, Hori Y, et al. A chandelier-illuminated anterior chamber maintainer for use during Descemet stripping automated endothelial keratoplasty in patients with advanced bullous keratopathy. *Cornea*. 2010;29:917–920.
11. Oshima Y, Awh CC, Tano Y. Self-retaining 27-gauge transconjunctival chandelier endoillumination for panoramic viewing during vitreous surgery. *Am J Ophthalmol*. 2007;143:166–167.
12. Oshima Y, Shima C, Maeda N, et al. Chandelier retroillumination-assisted torsional oscillation for cataract surgery in patients with severe corneal opacity. *J Cataract Refract Surg*. 2007;33:2018–2022.
13. Covert DJ, Koenig SB. New triple procedure: Descemet's stripping and automated endothelial keratoplasty combined with phacoemulsification and intraocular lens implantation. *Ophthalmology*. 2007;114:1272–1277.
14. Price FW Jr, Price MO. Endothelial keratoplasty to restore clarity to a failed penetrating graft. *Cornea*. 2006;25:895–899.
15. Kymionis GD, Suh LH, Dubovy SR, et al. Diagnosis of residual Descemet's membrane after Descemet's stripping endothelial keratoplasty with anterior segment optical coherence tomography. *J Cataract Refract Surg*. 2007;33:1322–1324.
16. Suh LH, Dawson DG, Mutapcic L, et al. Histopathologic examination of failed grafts in Descemet's stripping with automated endothelial keratoplasty. *Ophthalmology*. 2009;116:603–608.

TISSUE ENGINEERING: Part A
Volume 17, Numbers 17 and 18, 2011

DOI: 10.1089/ten.tea.2010.0568

# A Novel Gelatin Hydrogel Carrier Sheet for Corneal Endothelial Transplantation

Ryou Watanabe, M.D., Ph.D.,[1] Ryuhei Hayashi, Ph.D.,[2] Yu Kimura, Ph.D.,[3] Yuji Tanaka, Ph.D.,[4] Tomofumi Kageyama, M.S.,[2] Susumu Hara, Ph.D.,[2] Yasuhiko Tabata, Ph.D., D.Med.Sci., D.Pharm.,[3] and Kohji Nishida, M.D., Ph.D.[2]

We examined the feasibility of using gelatin hydrogels as carrier sheets for the transplantation of cultivated corneal endothelial cells. The mechanical properties, transparency, and permeability of gelatin hydrogel sheets were compared with those of atelocollagen sheets. Immunohistochemistry (ZO-1, $Na^+/K^+$-ATPase, and N-cadherin), hematoxylin and eosin staining, and scanning electron microscopy were performed to assess the integrity of corneal endothelial cells that were cultured on gelatin hydrogel sheets. The gelatin hydrogel sheets displayed greater transparency, elastic modulus, and albumin permeability compared to those of atelocollagen sheets. The corneal endothelial cells on gelatin hydrogel sheets showed normal expression levels of ZO-1, $Na^+/K^+$-ATPase, and N-cadherin. Hematoxylin and eosin staining revealed the formation of a continuous monolayer of cells attached to the gelatin hydrogel sheet. Scanning electron microscopy observations showed that the corneal endothelial cells were arranged in a regular, mosaic, and polygonal pattern with normal cilia. These results indicate that the gelatin hydrogel sheet is a promising material to transport corneal endothelial cells during transplantation.

## Introduction

THE CORNEAL ENDOTHELIUM is a monolayer of flattened hexagonal cells that line the posterior surface of the cornea. The physiological function of the corneal endothelium is to control the water content of the corneal stroma.[1] When corneal endothelial cells are damaged and their cell density is decreased by Fuchs' dystrophy, inflammation, or laser iridotomy, the human corneal endothelium does not regenerate naturally because the cells lack the ability to proliferate *in vivo*.[2,3] Consequently, the cornea cannot control stromal hydration, which can lead to bullous keratopathy (BK).

Penetrating keratoplasty (PKP) is the principal surgical procedure employed to treat BK. Recently, an alternative operative procedure, Descemet's stripping endothelial keratoplasty (DSEK), which is an endothelial keratoplasty, was developed.[4–6] In contrast to PKP, in DSEK, only the complex consisting of Descemet's membrane and the endothelium is removed from the recipient cornea, and the donor complex containing the thin corneal stroma, Descemet's membrane, and the endothelium are transplanted. The advantages of DSEK are fewer suture-related graft complications, decreased astigmatism, better visual acuity, and safer closed-eye surgery. Furthermore, DSEK is sufficient for most patients who have BK without opacity of the corneal stroma.

Millions of patients around the world require corneal transplantation. However, most patients are waiting for PKP or DSEK because of the shortage of donor corneas. Recently, it has become possible to cultivate human corneal endothelial cells (HCECs) *in vitro*. However, the thickness of the corneal endothelial layer is only 5 μm. Therefore, it is impossible to handle the HCECs during surgery without the use of carrier materials.

Some research groups use collagen sheets as a carrier for the cultivated corneal endothelial cells.[7,8] However, some characteristics of this material need improvement, such as its decreased transparency under wet conditions. Gelatin—the denatured form of collagen—has been used extensively as a biomaterial for pharmaceutical and medical applications because of its appropriate biodegradability[9] and biocompatibility in physiological environments.[10] Gelatin is used as an ingredient in drug formulations, as a sealant for vascular prostheses, and as a delivery vehicle.[11–14] In the present study, we examine gelatin hydrogels used as carrier sheets for the transplantation of cultivated HCECs.

[1]Department of Ophthalmology, Tohoku University Graduate School of Medicine, Sendai, Japan.
[2]Department of Ophthalmology, Osaka University School of Medicine, Suita, Japan.
[3]Department of Biomaterials, Institute for Frontier Medical Sciences, Kyoto University, Kyoto, Japan.
[4]Institute of Advanced Biomedical Engineering and Science, Tokyo Women's Medical University, Tokyo, Japan.

## Materials and Methods

### Materials

Gelatin hydrogel sheets processed through an alkaline treatment of porcine skin were prepared by dehydrothermal cross-linking. The mechanism of dehydrothermal cross-linking is that the functional groups are combined each other by being left out water.

An aqueous gelatin solution was poured into a polypropylene dish and dried at room temperature for 72 h. The dried gelatin sheets were then placed in a vacuum-drying oven (DN-30S; Sato Vac, Tokyo, Japan) at 160°C for 6, 12, 24, or 48 h under 0.01 Torr. Atelocollagen sheets fabricated from the collagen of bovine skin were purchased from KOKEN Co., Ltd. (Tokyo, Japan). The thickness of each sheet under wet conditions was 50 μm.

### Transparency measurement

The light transmission measurement was performed as described previously.[15] Briefly, the light transmission of the gelatin hydrogel and atelocollagen sheets was examined at room temperature using UV/vis spectroscopy (UV-2550/2450; SHIMADZU, Kyoto, Japan) for narrow spectral regions (centered at 400, 450, 500, 550, 600, 650, and 700 nm). Each sample was measured five times.

### Measurement of mechanical properties

The tensile strength, elongation at break, and elastic modulus of the gelatin hydrogel and atelocollagen sheets were determined as described previously.[16] Briefly, we used a Table-Top Universal Testing Instrument (EZ-S; SHIMADZU, Kyoto, Japan) at a rate of 100 mm/min. The results for measured region were recorded using TRAPEZIUM X software. Each sample was measured five times.

### Measurement of diffusion permeability using glucose and albumin

The diffusion permeability studies were carried out as previously described.[17] Briefly, we examined diffusion permeability using a two-compartment diffusion chamber system with a stir bar (Side-Bi-Side Cells; PermeGear, Inc., Hellertown, PA) at 35°C. Gelatin hydrogel sheets prepared by dehydrothermal cross-linking for 48 h and atelocollagen sheets (both 50-μm thick) were placed between the donor chamber and the receptor chamber, which was filled with phosphate-buffered saline (PBS; Invitrogen, Carlsbad, CA). The donor chamber was filled with either a 0.05 g/mL glucose solution or a 50 μM solution of fluorescein isothiocyanate-labeled human albumin (Sigma-Aldrich, St. Louis, MO). The solution in the receptor chamber was sampled and measured by spectrophotometric analysis (SpectraMax M2e-TG; Molecular Devices Inc., Sunnyvale, CA) using a glucose assay kit (Sigma-Aldrich). A fluorophotometric analysis (ARVO™ ×4; PerkinElmer Inc., Waltham, MA) of the fluorescein isothiocyanate-labeled albumin was performed (495-nm excitation, 519-nm emission). Each sample was measured three times.

### Primary cultures of HCECs

Human donor corneoscleral buttons for research were provided by Sightlife (Northwest Lions Eye Bank, Seattle, WA). All the corneas were preserved in Optisol-GS (Bausch & Lomb, Inc., Rochester, NY) within 1 day after death. The ages of the donors ranged from 19 to 52 years (n = 4), and the mean corneal endothelial cell density was 2999 ± 225 cells/mm$^2$. We used the four corneal donors in mixture.

Descemet's membrane with the endothelium was positioned with the endothelial cell side facing down onto 35-mm culture dishes coated with type IV collagen (Nitta Gelatin Inc., Osaka, Japan) and placed in an incubator (37°C and 10% $CO_2$). The concentration of type IV collagen solution was 0.3 mg/mL.

The culture medium, which consisted of Dulbecco's modified Eagle's medium (Nikken-Seibutsuigaku Laboratory, Kyoto, Japan) supplemented with 10% fetal bovine serum (Japan Bio serum, Hiroshima, Japan), 100 units/mL of penicillin, 100 μg/mL of streptomycin, and 2 ng/mL of basic fibroblast growth factor (Invitrogen), was changed three times per week. Beginning 4 weeks after seeding, the cells were trypsinized (0.25% Trypsin-EDTA; Invitrogen) and subcultured at a 1:2 dilution at each passage.

### Seeding of HCECs on the gelatin hydrogel sheet

Passage 3–4 confluent, subcultured cells derived from each of the human corneas were seeded onto gelatin hydrogel sheets coated with type IV collagen and the atelocollagen sheet as a control. The seeded cell density was 3–5 × 10$^3$ cells/mm$^2$, and the cells were cultivated for 3 weeks.

### Immunohistochemistry

HCECs on the atelocollagen and the gelatin hydrogel sheets prepared by dehydrothermal cross-linking for 48 h were used for immunohistochemistry, hematoxylin and eosin (HE) staining, and scanning electron microscopy (SEM).

**ZO-1 and N-cadherin.** The HCECs on each sheet were fixed at room temperature using 4% paraformaldehyde for 10 min and washed with Tris-buffered saline (TBS; Takara Bio Inc., Otsu, Japan) three times. The sheets were incubated overnight at 4°C with a 1:100 dilution of anti-ZO-1 antibody (1A12; Invitrogen) or anti-N-cadherin antibody (3B9; Invitrogen).

**$Na^+/K^+$-ATPase.** The HCECs on each sheet was fixed at −20°C with cold methanol for 10 min and washed with TBS three times. The sheets were incubated overnight with a 1:100 dilution of anti-$Na^+/K^+$-ATPase antibody (C464.6; Millipore, Billerica, MA) at 4°C. After primary antibody staining the sheets were again washed twice with TBS and then incubated with a 1:200 dilution of Alexa Fluor 488– or 568–conjugated secondary antibodies (Invitrogen). Finally, both of the gelatin sheets were counterstained with Hoechst 33342 (Invitrogen) and observed using confocal laser scanning microscopy (LSM 710; Carl Zeiss, Jena, Germany). For all immunostaining experiments, slides treated with isotype-matched nonspecific IgG antibodies were used as isotype controls.

### HE staining

Frozen 10-μm-thick sections of HCECs on the gelatin hydrogel sheet were embedded using OCT (Tissue-Tek; Sakura Fine Tek, Torrance, CA) and stained with HE.

*Electron microscopy*

HCECs on the gelatin hydrogel and the atelocollagen sheets were fixed with PBS containing 2% glutaraldehyde at 37°C for 1 h and washed three times with PBS. Subsequently, the cell sheets were fixed in 1% osmium tetroxide at room temperature for 1 h and then dehydrated through a graded series of ethanol concentrations. Next, the specimens were dried in a Critical Point Dryer (HCP-2; HITACHI, Ibaraki, Japan), coated with osmium using an osmium coater (HPC-30W; Vacuum Device Inc., Ibaraki, Japan), and observed with an SEM (S-3200H; HITACHI) at 5 kV.

*Statistical analysis*

The data are expressed as the mean ± standard deviation. Differences in the mean transparency and mean mechanical properties between the gelatin hydrogel groups and the control (i.e., atelocollagen) group were analyzed using the Dunnett test. Differences among the mean transparencies of the gelatin hydrogel groups were analyzed using the Kruskal–Wallis test. Differences in the diffusion permeability were measured using Student's *t*-test. All the statistics were calculated using SigmaStat 3.5 (Systat Software Inc., Point Richmond, CA). *p*-values $< 0.05$ were considered statistically significant.

## Results

In the present experiment, we characterized the properties of gelatin hydrogen sheets and used atelocollegen sheets as a control.

*Transparency measurement*

Figure 1A shows the appearance of the gelatin hydrogel and atelocollagen sheets. The mean light transmissions of the gelatin hydrogels prepared by dehydrothermal cross-linking for 6, 12, 24, and 48 h were 99.1% ± 0.1%, 99.0% ± 0.2%, 98.8% ± 0.5%, and 99.0% ± 0.6%, respectively. The mean light transmission of atelocollagen was 72.1% ± 2.1% (Fig. 1B). All the gelatin hydrogel sheets were clear at each of the wavelengths tested and demonstrated better light transmission properties compared with the atelocollagen ($p < 0.05$). Among the gelatin hydrogel sheet groups, no statistically significant differences in transparency were observed ($p = 0.826$), and the degree of transparency did not depend on the cross-linking time.

*Measurement of mechanical properties*

The mechanical properties of the gelatin hydrogel sheets were compared with those of the atelocollagen sheets (Fig. 2). Figure 2A shows an example of the measurement of mechanical properties. In the gelatin hydrogels, the tensile strength and elastic modulus increased with longer dehydrothermal cross-linking times (Fig. 2B and D). The elongation at break, however, decreased with longer dehydrothermal cross-linking time (Fig. 2C). The gelatin hydrogels generated by dehydrothermal cross-linking for 24 and 48 h were significantly better than those made from atelocollagen with respect to the tensile strength and elongation at break ($p < 0.05$). Additionally, the gelatin hydrogels generated by dehydrothermal cross-linking for 48 h exhibited a significantly greater elastic modulus compared to those made from atelocollagen ($p < 0.05$). These results demonstrate that the mechanical properties of atelocollagen are similar to those of gelatin hydrogels prepared by dehydrothermal cross-linking for 6 h.

*Measurement of the diffusion permeability*

The results of the diffusion permeability measurements are summarized in Figure 3. The albumin diffusion coefficient for the gelatin hydrogels (diffusion permeability $D = 9.67 \pm 1.46 \times 10^{-8}$ cm$^2$/s) was about twice the value obtained for atelocollagen ($D = 5.13 \pm 1.82 \times 10^{-8}$ cm$^2$/s) ($p < 0.05$) (Fig. 3A). In contrast, the glucose diffusion permeability test revealed similar diffusion permeabilities for gelatin hydrogels ($D = 2.55 \pm 0.11 \times 10^{-7}$ cm$^2$/s) and atelocollagen ($D = 2.55 \pm 0.02 \times 10^{-7}$ cm$^2$/s) ($p = 0.962$) (Fig. 3B).

A

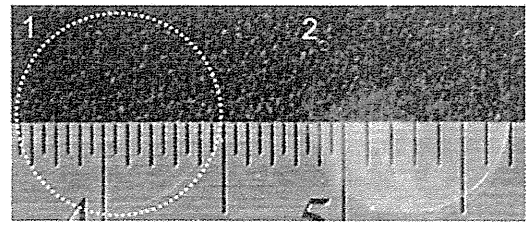


1; gelatin hydrogel sheet
(dehydrothermal cross-linking time; 48hr)
2; atelocollagen sheet

B

| | | Gelatin hydrogel (hr = dehydrothermal cross-linking time) | | | |
|---|---|---|---|---|---|
| | atelocollagen | 6hr | 12hr | 24hr | 48hr |
| Transmission (%) | 72.1 ± 2.1 | 99.1±0.1 * | 99.0 ± 0.2 * | 98.8 ± 0.5 * | 99.0 ± 0.6 * |

FIG. 1. (A) The appearance of gelatin hydrogel and atelocollagen under wet conditions. (B) The table shows the transparency measurements. The data are presented as the means (400–700 nm) ± SD (*, $p < 0.05$). SD, standard deviation.

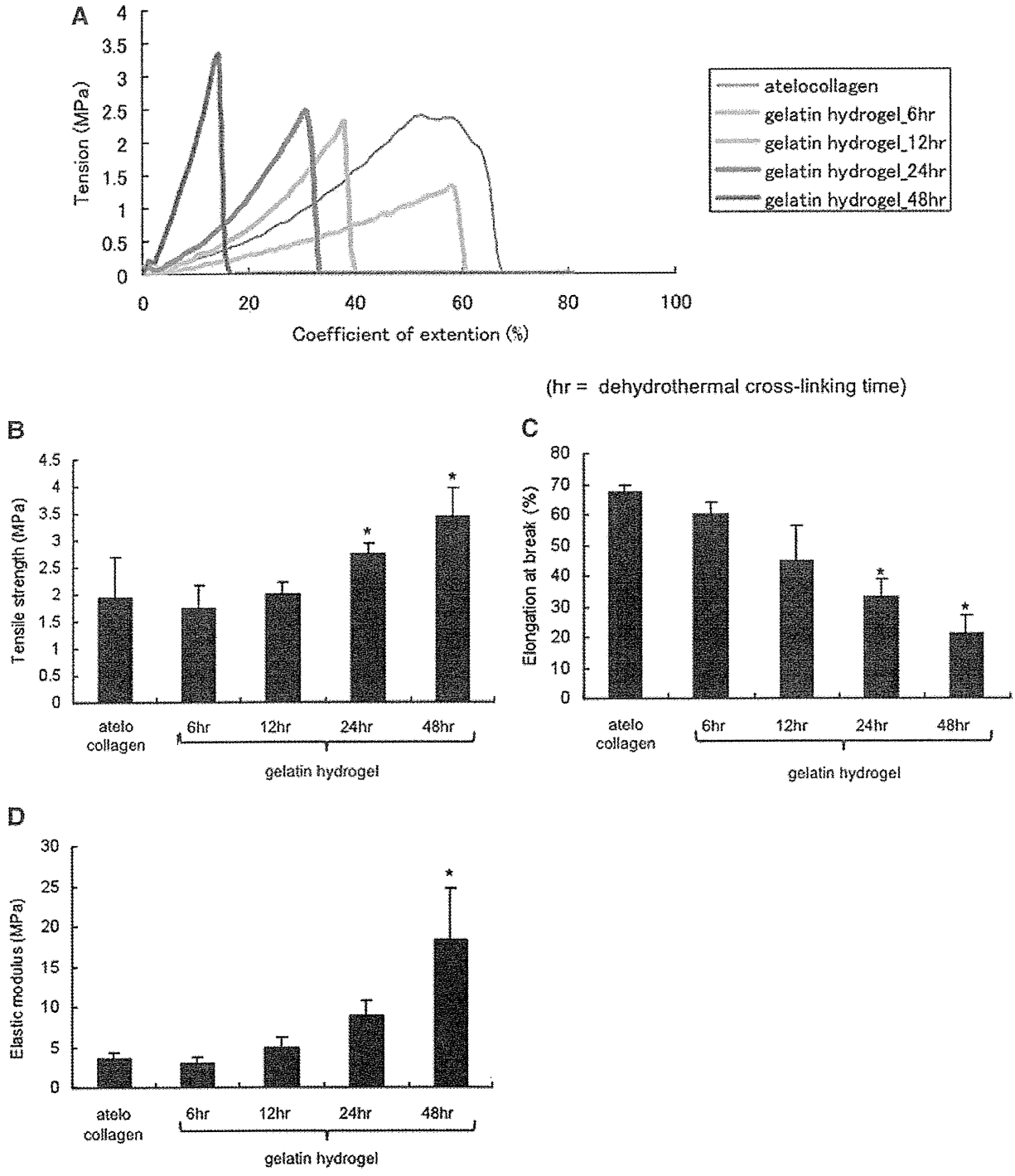


FIG. 2. **(A)** The upper graph shows an example of the measurement of mechanical properties. The lower graphs present the results obtained for the tensile strength **(B)**, elongation at break **(C)**, and elastic modulus tests **(D)**. The gelatin hydrogel sheet was compared with the atelocollagen sheet. Error bars indicate the SD, and the data are presented as means ± SD (*, $p < 0.05$).

*Immunohistochemistry*

The immunostaining for $Na^+/K^+$-ATPase, ZO-1, and N-cadherin in HCECs on the gelatin hydrogel and the atelocollagen are shown in Figure 4. The $Na^+/K^+$-ATPase, which regulates the ion balance to maintain the proper physiological function of the corneal endothelium, was present at the cell boundaries. ZO-1, the peripheral membrane phosphoprotein associated with tight junctions, was localized to the intercellular face of the cultivated HCECs. N-cadherin

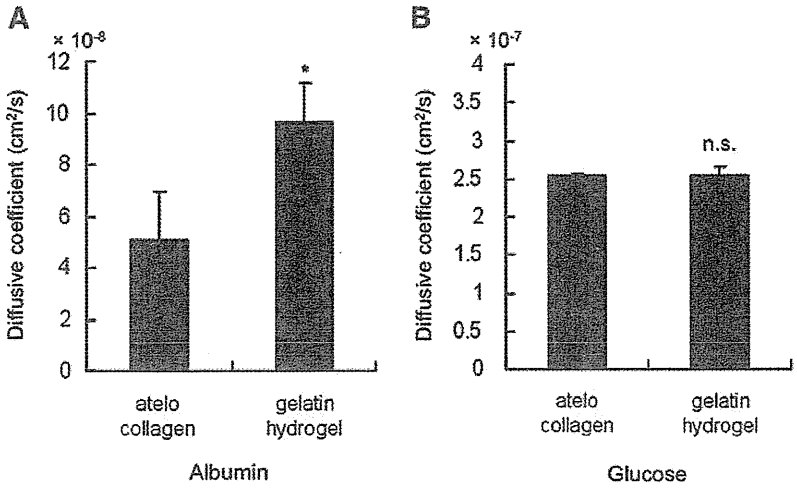


FIG. 3. Comparison of the diffusion permeabilities to albumin (A) and glucose (B) between the gelatin hydrogel and atelocollagen. Gelatin hydrogels were prepared by dehydrothermal cross-linking for 48 h. Error bars indicate the SD, and the data are presented as means ± SD (*, $p < 0.05$). n.s., not significant.

was similarly localized to the intercellular region in both cultivated HCECs on the gelatin hydrogel and the atelocollagen sheet.

### *HE staining*

HE staining showed that the cultivated HCECs were existed as a continuous monolayer and attached to the gelatin hydrogel (Fig. 5A).

### *Electron microscopy*

The SEM observations demonstrated that the cultivated HCECs on both the gelatin hydrogel and atelocollagen sheets were arranged in a regular mosaic pattern with ruffled borders (Fig. 5B). The HCECs tightly approximated the lateral plasma membrane of the adjacent endothelial cells. Natural cilia were observed on the cell surfaces of both cultivated HCECs on the gelatin hydrogel and atelocollagen sheets.

## Discussion

The present study demonstrates that gelatin hydrogel sheets prepared by dehydrothermal cross-linking are suitable as carrier sheets for corneal endothelial transplantation and that they are superior to atelocollagen sheets. The transparency of all the gelatin hydrogel sheets was nearly 100%, which is significantly higher than the transparency of atelocollagen. The elastic modulus of the gelatin hydrogel was ~5-fold higher than that of atelocollagen. Moreover, the albumin diffusion coefficient for the gelatin hydrogels was approximately twice that of atelocollagen. These results indicate that gelatin hydrogels possess the appropriate characteristics for use as carriers in corneal endothelial cell sheet transplantation.

It is essential that the carrier for the corneal endothelial sheet be transparent. In this study, we compared the transparency of gelatin hydrogel and atelocollagen sheets. The gelatin hydrogels were far more transparent than the atelocollagen sheets. The gelatin hydrogel sheets prepared by dehydrothermal cross-linking for 48 h demonstrated a greater stiffness but a lower elongation and load at break as compared with atelocollagen sheets, indicating that the gelatin hydrogel sheets are suitable carriers because they might reduce the risk of damage to the corneal endothelial cell sheets. Our data also suggest that gelatin hydrogel sheets possess sufficient mechanical strength for transplantation.

Glucose and albumin, which are essential for the maintenance of corneal health, are supplied primarily via the aqueous humor and, to a lesser extent, through the limbal vasculature.[18] The albumin permeability of the gelatin hydrogel was approximately twice that of atelocollagen. High permeability is a major advantage for corneal endothelial carriers. The cultivated HCECs on both gelatin hydrogel and atelocollagen sheets displayed normal expression patterns of ZO-1, $Na^+/K^+$-ATPase, and N-cadherin proteins. Furthermore, the SEM observations revealed that the HCECs on the gelatin hydrogel were polygonal and had specific structures, similar to their morphologies *in vivo* and on the atelocollagen sheet.[1] These results from immunohistochemical and morphological analyses between the gelatin hydrogel and atelocollagen gel sheets were largely similar. This suggests that the gelatin hydrogel sheet is capable of supporting the function of the corneal endothelial sheet prepared *in vitro* similar to the atelocollagen sheet.

In the present study we used atelocollagen sheet as a control because it has already been used for transplantation of cultured HCECs to disease model of monkey.[7] The atelocollagen sheet is thought to be candidate material for clinical use even though it has problems to solve. Our ultimate goal is clinical application; therefore, we consider that the atelocollagen sheet is the most adequate material as a control.

There have been previous reports of the use of biomaterials, including gelatin hydrogels and hyaluronic acid as corneal endothelial cell sheet carriers.[19–22] In contrast to our method, Jumblatt *et al.* and McCulley *et al.* used gelatin hydrogels that were cross-linked with glutaraldehyde, which may have harmful effects on the human body. Moreover, they examined only rabbit corneal endothelial cells, which have a higher proliferative ability than HCECs. Our sheets have been designed for eventual use in clinical applications, and therefore it is essential that the HCECs proliferate naturally on the gelatin hydrogel sheet. In addition, Hsiue *et al.*[19] used a thick gelatin disc with a higher elastic modulus

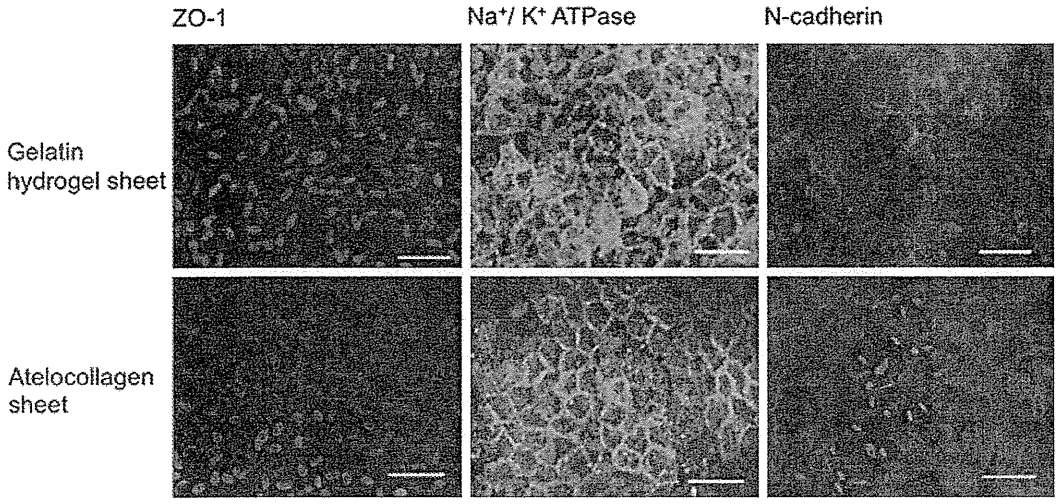


FIG. 4. Immunohistochemistry of human corneal endothelial cells on the gelatin hydrogel and atelocollagen sheets for $Na^+/K^+$ ATPase, ZO-1, and N-cadherin. Scale bar, 50 μm. Each gelatin hydrogel sheet was prepared by dehydrothermal cross-linking for 48 h.

than that described for our sheet. However, it is preferable to use as little material from outside as possible. In the present study, we successfully generated thin gelatin hydrogel sheets with sufficient mechanical strength and transparency in the absence of a cross-linking reagent. Thus, our gelatin hydrogel sheets have an advantage in terms of thickness, the cross-linking method, and transparency, as compared to other carriers. Because our final goal is to develop carrier sheet, which is available for clinical application, we believe that the cross-linking method and the transparency of the gelatin hydrogel sheet are of advantage. Regarding hyaluronic acid, we actually seeded the cultivated corneal endothelial cells on the sheet made from hyaluronic acid. However, corneal endothelial cells were not able to adhere to hyaluronic acid sheet tightly (data not shown).

## Conclusion

In this study, we demonstrated the suitability of a new candidate for carrying HCECs. Gelatin hydrogel sheet has benefits over atelocollagen, including higher transparency, elastic modulus, and albumin diffusion permeability. More-

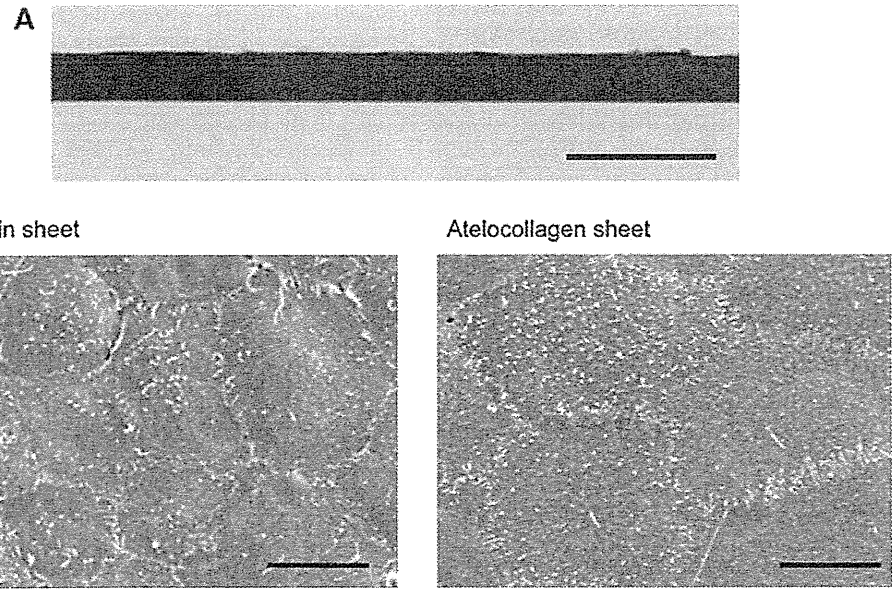


FIG. 5. **(A)** Hematoxylin and eosin staining of the corneal endothelial cells on the gelatin hydrogel and atelocollagen sheets. Scale bar, 50 μm. **(B)** Observation of human corneal endothelial cells on the gelatin hydrogel and atelocollagen sheets by using scanning electron microscope. Scale bar, 15 μm. Gelatin hydrogel sheet was prepared by dehydrothermal cross-linking for 48 h.

over, the cultivated HCECs on the gelatin hydrogel sheet are same as normal HCECs *in vivo*. Our findings suggest that gelatin hydrogels have appropriate characteristics to be used as carrier sheets for corneal endothelial transplantation.

## Acknowledgments

This work was supported in part by Grants-in-Aid for Scientific Research from the Ministry of Health, Labor and Welfare and from National Institute of Biomedical Innovation in Japan.

## Disclosure Statement

No competing financial interests exist.

## References

1. Waring, G.O., 3rd, Bourne, W.M., Edelhauser, H.F., and Kenyon, K.R. The corneal endothelium. Normal and pathologic structure and function. Ophthalmology **89,** 531, 1982.
2. Joyce, N.C., Navon, S.E., Roy, S., and Zieske, J.D. Expression of cell cycle-associated proteins in human and rabbit corneal endothelium *in situ*. Invest Ophthalmol Vis Sci **37,** 1566, 1996.
3. Joyce, N.C., Meklir, B., Joyce, S.J., and Zieske, J.D. Cell cycle protein expression and proliferative status in human corneal cells. Invest Ophthalmol Vis Sci **37,** 645, 1996.
4. Price, M.O., Giebel, A.W., Fairchild, K.M., and Price, F.W., Jr. Descemet's membrane endothelial keratoplasty: prospective multicenter study of visual and refractive outcomes and endothelial survival. Ophthalmology **116,** 2361, 2009.
5. Price, M.O., and Price, F.W. Descemet's stripping endothelial keratoplasty. Curr Opin Ophthalmol **18,** 290, 2007.
6. Terry, M.A. Endothelial keratoplasty: history, current state, and future directions. Cornea **25,** 873, 2006.
7. Koizumi, N., Sakamoto, Y., Okumura, N., Okahara, N., Tsuchiya, H., Torii, R., Cooper, L.J., Ban, Y., Tanioka, H., and Kinoshita, S. Cultivated corneal endothelial cell sheet transplantation in a primate model. Invest Ophthalmol Vis Sci **48,** 4519, 2007.
8. Mimura, T., Yamagami, S., Yokoo, S., Usui, T., Tanaka, K., Hattori, S., Irie, S., Miyata, K., Araie, M., and Amano, S. Cultured human corneal endothelial cell transplantation with a collagen sheet in a rabbit model. Invest Ophthalmol Vis Sci **45,** 2992, 2004.
9. Balakrishnan, B., and Jayakrishnan, A. Self-cross-linking biopolymers as injectable *in situ* forming biodegradable scaffolds. Biomaterials **26,** 3941, 2005.
10. Yao, C.H., Liu, B.S., Hsu, S.H., Chen, Y.S., and Tsai, C.C. Biocompatibility and biodegradation of a bone composite containing tricalcium phosphate and genipin crosslinked gelatin. J Biomed Mater Res A **69,** 709, 2004.
11. Takemoto, Y., Kawata, H., Soeda, T., Imagawa, K., Somekawa, S., Takeda, Y., Uemura, S., Matsumoto, M., Fujimura, Y., Jo, J., Kimura, Y., Tabata, Y., and Saito, Y. Human placental ectonucleoside triphosphate diphosphohydrolase gene transfer via gelatin-coated stents prevents in-stent thrombosis. Arterioscler Thromb Vasc Biol **29,** 857, 2009.
12. Hashimoto, T., Koyama, H., Miyata, T., Hosaka, A., Tabata, Y., Takato, T., and Nagawa, H. Selective and sustained delivery of basic fibroblast growth factor (bFGF) for treatment of peripheral arterial disease: results of a phase I trial. Eur J Vasc Endovasc Surg **38,** 71, 2009.
13. Patel, Z.S., Ueda, H., Yamamoto, M., Tabata, Y., and Mikos, A.G. *In vitro* and *in vivo* release of vascular endothelial growth factor from gelatin microparticles and biodegradable composite scaffolds. Pharm Res **25,** 2370, 2008.
14. Ito, N., Saito, S., Yamada, M.H., Koizuka, S., Obata, H., Nishikawa, K., and Tabata, Y. A novel bFGF-GH injection therapy for two patients with severe ischemic limb pain. J Anesth **22,** 449, 2008.
15. Merrett, K., Fagerholm, P., McLaughlin, C.R., Dravida, S., Lagali, N., Shinozaki, N., Watsky, M.A., Munger, R., Kato, Y., Li, F., Marmo, C.J., and Griffith, M. Tissue-engineered recombinant human collagen-based corneal substitutes for implantation: performance of type I versus type III collagen. Invest Ophthalmol Vis Sci **49,** 3887, 2008.
16. Liu, W., Merrett, K., Griffith, M., Fagerholm, P., Dravida, S., Heyne, B., Scaiano, J.C., Watsky, M.A., Shinozaki, N., Lagali, N., Munger, R., and Li, F. Recombinant human collagen for tissue engineered corneal substitutes. Biomaterials **29,** 1147, 2008.
17. Liu, Y., Gan, L., Carlsson, D.J., Fagerholm, P., Lagali, N., Watsky, M.A., Munger, R., Hodge, W.G., Priest, D., and Griffith, M. A simple, cross-linked collagen tissue substitute for corneal implantation. Invest Ophthalmol Vis Sci **47,** 1869, 2006.
18. DiMattio, J. *In vivo* entry of glucose analogs into lens and cornea of the rat. Invest Ophthalmol Vis Sci **25,** 160, 1984.
19. Hsiue, G.H., Lai, J.Y., Chen, K.H., and Hsu, W.M. A novel strategy for corneal endothelial reconstruction with a bioengineered cell sheet. Transplantation **81,** 473, 2006.
20. McCulley, J.P., Maurice, D.M., and Schwartz, B.D. Corneal endothelial transplantation. Ophthalmology **87,** 194, 1980.
21. Jumblatt, M.M., Maurice, D.M., and Schwartz, B.D. A gelatin membrane substrate for the transplantation of tissue cultured cells. Transplantation **29,** 498, 1980.
22. Lu, P.L., Lai, J.Y., Ma, D.H., and Hsiue, G.H. Carbodiimide cross-linked hyaluronic acid hydrogels as cell sheet delivery vehicles: characterization and interaction with corneal endothelial cells. J Biomater Sci Polym Ed **19,** 1, 2008.

Address correspondence to:
*Kohji Nishida, M.D., Ph.D.*
*Department of Ophthalmology*
*Osaka University Medical School*
*Rm. E7, 2-2 Yamadaoka*
*Suita, Osaka 565-0871*
*Japan*

*E-mail:* knishida@ophthal.med.osaka-u.ac.jp

*Received: September 27, 2010*
*Accepted: April 29, 2011*
*Online Publication Date: July 7, 2011*

Genes to Cells

# Neural crest-derived multipotent cells in the adult mouse iris stroma

Miki Kikuchi[1], Ryuhei Hayashi[1], Sachiko Kanakubo[1,2], Ayumi Ogasawara[2], Masayuki Yamato[3], Noriko Osumi[2] and Kohji Nishida[1]*

[1]*Department of Ophthalmology, Tohoku University School of Medicine, Sendai, Japan*
[2]*Division of Developmental Neuroscience, Center for Translational and Advanced Animal Research, Tohoku University School of Medicine, 1-1 Seiryomachi, Aoba-ku, Sendai 980-8574, Japan*
[3]*Institute of Advanced Biomedical Engineering and Science, Tokyo Women's Medical University, Tokyo, Japan*

**The purpose of this study was to characterize neural crest–derived cells within the adult murine iris. The iris was isolated from P0-Cre/Floxed-EGFP transgenic (TG) mice. The isolated iris cells formed EGFP-positive spheres on non-adhesive culture plates. Immunostaining showed that these EGFP-positive spheres expressed neural crest markers including Sox10 and p75NTR, and these cells showing *in vitro* sphere-forming ability were originally resided in the iris stroma (IS), *in vivo*. Real-time RT-PCR showed that the EGFP-positive spheres expressed significantly higher levels of the neural crest markers than EGFP-negative spheres and bone marrow–derived mesenchymal stem cells. Furthermore, the iris stromal sphere had capability to differentiate into various cell lineages including smooth muscle and cartilage. These data indicate that neural crest–derived multipotent cells can be isolated from the murine IS and expanded in sphere culture.**

## Introduction

During development, the neural crest generates various cell types in adult vertebrate organisms, including cells that give rise to the autonomic nervous system, primary sensory neurons, smooth muscle of the cardiac outflow tract, melanocytes, cranial mesenchymal tissues, and some ocular tissues (Osumi-Yamashita *et al.* 1994; Le Douarin & Kalcheim 1999). Recent reports have showed that in adult tissues, neural crest–derived tissue-specific stem/progenitor cells are widely distributed, as they were observed in the skin, cardiac muscle, and corneal stroma (CS) (Toma *et al.* 2001; Tomita *et al.* 2005; Wang *et al.* 2006; Yoshida *et al.* 2006; Yu *et al.* 2006). These neural crest–derived cells have the capability to differentiate into multiple cell lineages originating from the neural crest. Therefore, these cells are thought to be 'neural crest stem cells' (Morrison *et al.* 1999; Dupin *et al.* 2007).

Previous embryonic developmental analyses using TG mouse and chicken embryos suggest that many of the ocular tissues originate from the cranial neural crest (Gage *et al.* 2005). Cranial neural crest–derived anterior segments of the eye are thought to develop in the following three steps (Saika *et al.* 2001; Jin *et al.* 2002). The first wave of neural crest cells differentiates to form the trabecular meshwork (TM) and corneal endothelium (CEnd). The second wave gives rise to CS cells, and the third wave contributes to the development of the iris. Among eye tissues that are from neural crest-originated cells, the iris is the only tissue that can be isolated by routine ophthalmological surgery. The iris therefore could be an excellent cell source for regenerative therapy of neural crest–originated ocular tissues. In this study, we report the isolation and characterization of neural crest–derived cells in the adult murine iris stroma (IS).

## Results

### Localization of cells derived from the neural crest in the anterior segment of the mouse eye

P0-Cre; EGFP mice were generated by crossing TG mice expressing Cre enzyme driven by the P0 promoter with *CAG-CAT-EGFP* TG line (Fig. 1A).

*Communicated by*: Masayuki Yamamoto (Tohoku University)
**Correspondence:* knishida@oph.med.tohoku.ac.jp

DOI: 10.1111/j.1365-2443.2011.01485.x

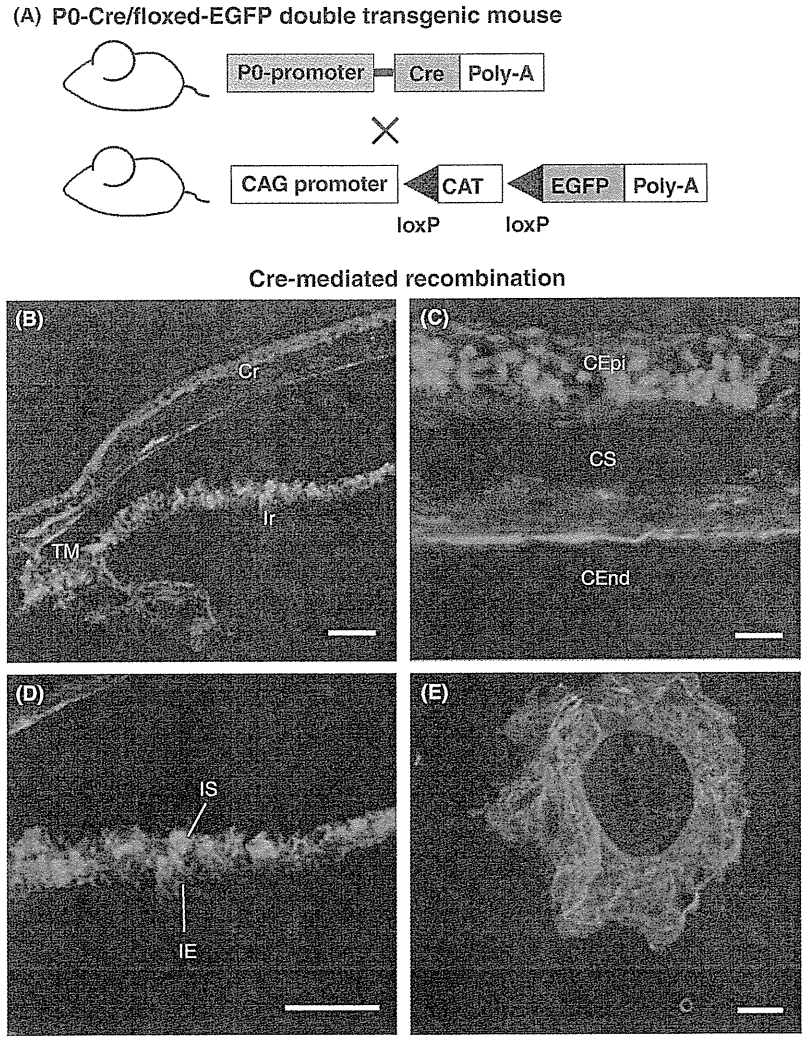


**Figure 1** Distribution of EGFP-positive cells in the anterior segment of the P0-Cre; EGFP mouse eye. Transgenic (TG) mice expressing the Cre enzyme driven by the myelin protein zero (P0) promoter were crossed with the TG line, *CAG-CAT-EGFP* (A). EGFP-labeled cells (green) were observed in the iris (Ir), trabecular meshwork and cornea (Cr) (B). Magnified view of (B) shows EGFP-positive cells localized in the corneal endothelium, part of the corneal stroma and the iris stroma (C–D). Isolated iris tissue was observed by fluorescent microscopy (E). IE, Iris pigment epithelium; CEpi, corneal epithelium. Scale bar: 100 μm (B, D), 20 μm (C), 400 μm (E).

Immunofluorescence staining showed that EGFP was expressed in the iris (Ir), TM, and cornea (Cr) (Fig. 1B). A magnified view of Fig. 1B shows that EGFP-positive cells were specifically localized in the CEnd, as well as part of the CS and the IS (Fig. 1C–D). EGFP expression was also observed in the whole area of irises enucleated from the eyes of P0-Cre; EGFP mice (Fig. 1E). These expression patterns confirmed data in the previous reports (Kanakubo *et al.* 2006; Yoshida *et al.* 2006).

### *In vivo* localization of Sox10 and p75NTR positive cells in the iris tissue of P0-Cre; EGFP mice

The expressions of Sox10 and p75NTR, typical neural crest markers, were examined in the iris tissue by Immunostaining. The result showed that both Sox10 and p75NTR were localized only in the iris stromal part (Fig. 2A–F). These neural crest markers were co-expressed with EGFP in the most part of iris stromal cells. The Immunofluorescent staining of

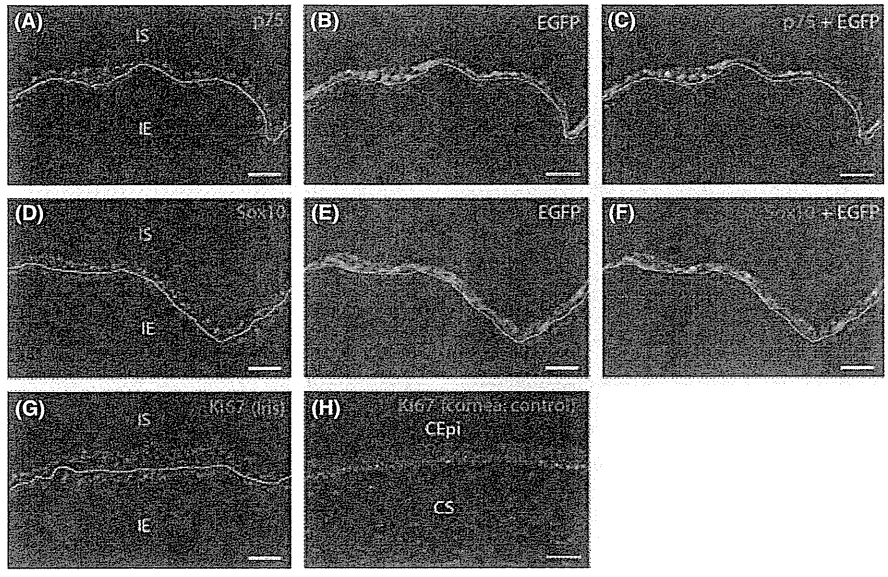


**Figure 2** *In vivo* localization of neural crest and proliferation markers in the iris of P0-Cre; EGFP mouse. The expressions of sox10 and p75NTR, typical neural crest markers, in the iris tissue were examined by immunostaining. Both p75NTR (A–C) and sox10 (D–F) were localized only in the iris stromal part. These neural crest markers were co-expressed with EGFP in the large part of iris stromal cells. The immunostaining of Ki67 showed that there was no Ki67-positive proliferating iris cell *in vivo* (G). Control slide showed that Ki-67 positive cells in existed in the basal layer of corneal epithelium (H). Scale bar: 50 μm.

a proliferation marker Ki67 indicated that there were almost no proliferating cells in the normal iris tissue *in vivo*. (Fig. 2G). Therefore, EGFP-positive neural crest–derived cells seem to be non-proliferative in the normal homeostatic condition.

### Sphere formation from iris cells of P0-Cre; EGFP mice

To characterize the EGFP-positive cells in the iris, we performed sphere formation assays. Iris cells isolated from P0-Cre; EGFP mice were cultured in non-adhesive culture plates. A number of EGFP-positive spheres were formed from the iris cells (Fig. 3A). Some of the EGFP-positive iris cells dissociated from the primary spheres had a capability to form secondary spheres (Fig. 3B). Supporting a previous report (Yoshida *et al.* 2006), it thus suggested that there are stem cell-like cells that can be grown in sphere culture in the iris cells.

### Immunostaining of stem cell and neural crest markers

Immunostaining showed that the spheres were composed of EGFP-positive iris stromal cells and expressed stem cell markers such as Nestin and Sox2 (Fig. 3C–E). They also expressed typical neural crest markers, such as Sox10, p75NTR, and AP-2β (Fig. 3F–H) (Kanakubo *et al.* 2006; Lee *et al.* 2007). Furthermore, BrdU assay showed that BrdU- and Ki67-positive cells existed in the iris spheres (Fig. 3I–J). This means that the sphere culture condition has successfully turned EGFP-positive dormant neural crest–derived cells into proliferative.

### Fluorescence activated cell sorting and gene expression analyses of stem cell and neural crest markers

Flow cytometric analysis showed that iris cells consisted of 39.8 ± 2.3% ($N = 6$) EGFP-positive iris stromal cells (Fig. 4A). Sphere culture showed that both isolated EGFP-positive and EGFP-negative cells could form spheres after 5 days of culture (Fig. 4B), and their sphere-forming efficiencies were 0.60 ± 0.079% and 0.46 ± 0.053%, respectively ($N = 5$). The harvested EGFP-positive iris stromal spheres expressed the stem cell markers Sox2, Nestin and Musashi1 as well as the neural crest makers Slug, p75NTR, Sox9, 10, AP-2α and β (Fig. 4C). Real-time RT-PCR showed that the EGFP-positive

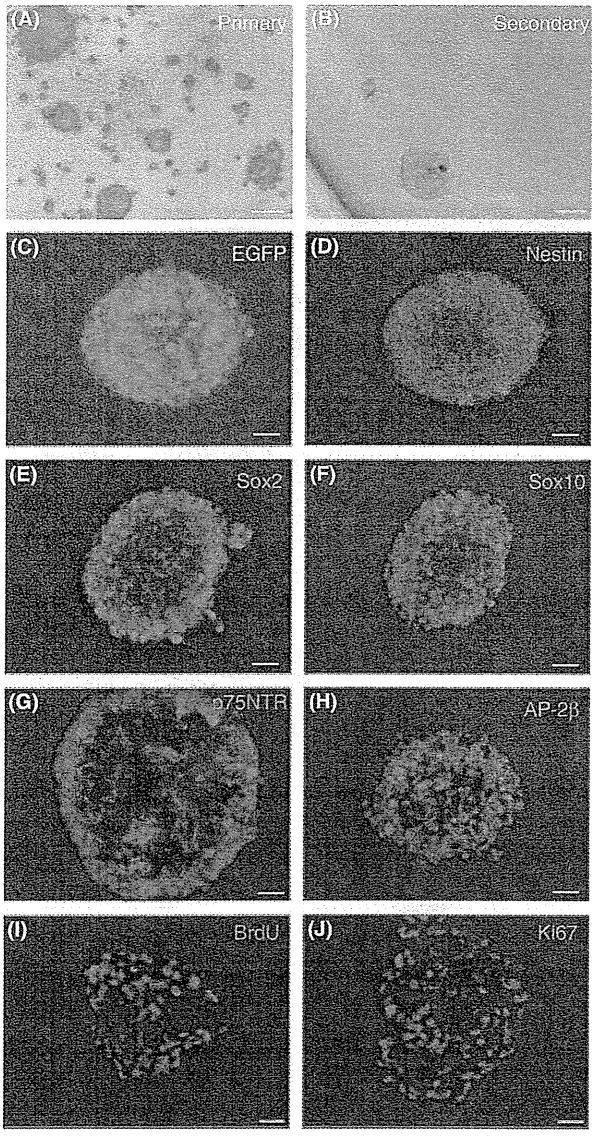


**Figure 3** Sphere culture and immunofluorescence staining of stem cell- and neural crest–related markers. Cells were isolated from iris tissue and then cultured in non-adhesive culture plates to form spheres. Microscopic observation showed that EGFP-positive spheres formed after 7 days of culture (A). A subset of EGFP-positive cells from primary spheres formed secondary spheres (B). Observation of frozen sections showed that almost all of the cells that composed the spheres were EGFP positive (C; green). Immunofluorescence staining showed that cells in EGFP-positive iris spheres expressed the stem cell markers Nestin and Sox2 (D–E; red), as well as the neural crest markers Sox10, p75NTR, and AP-2β (F–H; red). In addition, BrdU- and Ki67-positive proliferating cells existed in iris spheres (I–J; red). Nuclei were labeled with Hoechst 33342 (blue). Scale bar: 100 μm (A, B), 20 μm (C–J).

spheres expressed significantly higher levels of the neural crest markers Sox10, p75NTR, and AP-2β than EGFP-negative spheres or bone marrow–derived mesenchymal stem cells (MSCs) (Fig. 4D).

### Cell differentiation

To investigate the multipotency of the EGFP-positive iris stromal spheres, we performed differentiation assays for multiple neural crest cell lineages. EGFP-expressing cells migrated from the circumference of the spheres and co-expressed βIII-tubulin (11.5 ± 2.0%, $N = 8$), glial fibrillary acidic protein (GFAP) (28.8 ± 9.6%, $N = 4$) and alpha smooth muscle actin (αSMA) (74.0 ± 9.6%, $N = 4$) (Fig. 5A–F). Pellet cultures showed that most of the aggregated cells were stained with alcian blue and also expressed aggrecan and type II collagen (Fig. 5G–I), typical differentiation markers of chondrocytes. Statistical analyses of the differentiation efficiencies were shown in Table 1. These data suggest that EGFP-positive cells have potentials to differentiate into various cell types in cultures.

## Discussion

Our observation of the anterior segment of the P0-Cre; EGFP mouse eye showed EGFP-positive cells in the CEnd, TM, and IS. In contrast, there was no EGFP-positive cell in iris pigment epithelium and corneal epithelium that were generated from neural and surface ectoderm. These data support the previous reports that the P0-Cre; EGFP mouse allows accurate labeling of neural crest–derived tissues (Jin *et al.* 2002; Kanakubo *et al.* 2006; Yoshida *et al.* 2006). EGFP-positive cells isolated from the iris could form EGFP-positive spheres on non-adhesive culture plates. Secondary sphere culture showed that at least some iris stromal cells in the primary EGFP-positive iris spheres had the ability to reform spheres. Additionally, BrdU assay and Ki67 staining showed that a subgroup of BrdU- and Ki67-positive proliferating cells existed in the primary spheres, although there were no proliferating cells in the iris tissue *in vivo*. These findings suggest that the iris spheres are formed as a result of proliferation of the iris cells, rather than by aggregation.

Immunostaining of spheres for stem cell markers showed that EGFP-positive iris spheres expressed not only the stem cell markers generally expressed in various tissue-specific stem cells, i.e. Nestin, Musashi1, and Sox2, but also typical neural crest markers such as

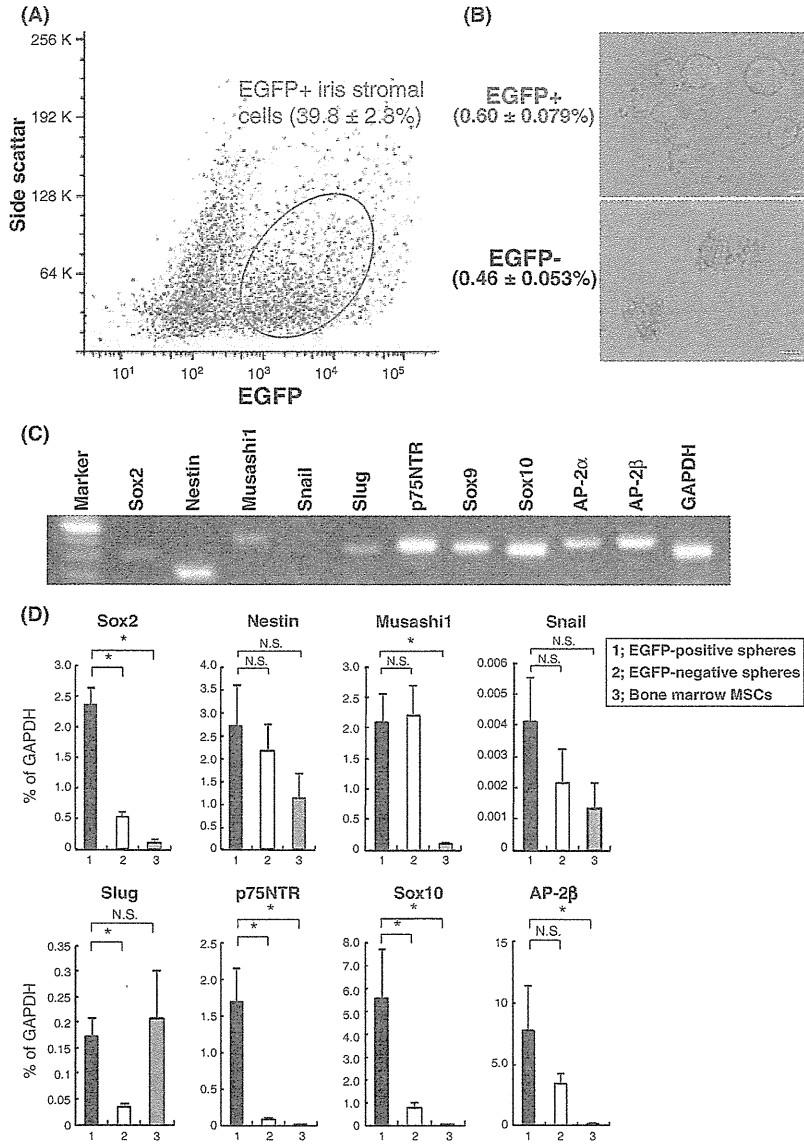


**Figure 4** FACS and gene expression analyses of stem cell and neural crest–related markers in iris stromal spheres. Isolated iris cells from P0-Cre; EGFP mice were submitted to FACS (A). The iris cells were composed of approximately 39.8 ± 2.3% (mean ± SE, $N = 6$) EGFP-positive cells. After 5 days of sphere culture, the isolated EGFP-positive and EGFP-negative cells formed each sphere (B). And their sphere-forming efficiencies were 0.60 ± 0.079% and 0.46 ± 0.053%, respectively (mean ± SE, $N = 5$). RT-PCR showed that the EGFP-positive spheres expressed the stem cell markers Nestin, Musashi1, and Sox2, as well as the neural crest markers Slug, p75NTR, Sox9, Sox10, and AP-2α and AP-2β (C). Real-time RT-PCR showed that the EGFP-positive spheres expressed significantly higher levels of neural crest marker genes, Sox10, p75NTR, and AP-2β than EGFP-negative spheres or mesenchymal stem cells (D). Scale bar: 50 μm. The graphs show the mean ± SE of 4–6 independent samples. *indicates $P < 0.05$.

p75NTR, AP-2β, and Sox10 (Morrison *et al.* 2000; Lee *et al.* 2007). Some of these markers, including Sox2 and Sox10, seemed to be expressed more strongly in the peripheral part of the spheres than in the central part. As it was previously reported, the differentiation status may be different between peripheral and central parts of the spheres (Campos 2004).